Available online at www.sciencedirect.com
SCIENCE DIRECT
Journal of Solid State Chemistry 179 (2006) 2133–2140
JOURNAL OF SOLID STATE CHEMISTRY
www.elsevier.com/locate/jssc

A series of spinel phase cathode materials prepared by a simple hydrothermal process for rechargeable lithium batteries

Yan-Yu Liang[a], Shu-Juan Bao[a], Hu-Lin Li[a,b,*]

[a]College of Chemistry and Chemical Engineering, Lanzhou University, Lanzhou, 730000, PR China
[b]College of Material Science and Engineering, Nanjing University of Aeronautics and Astronautics, Nanjing, 210016, PR China

Received 9 September 2005; received in revised form 25 March 2006; accepted 8 April 2006
Available online 25 April 2006

Abstract

A series of spinel-structured materials have been prepared by a simple hydrothermal procedure in an aqueous medium. The new synthetic method is time and energy saving i.e., no further thermal treatment and extended grinding. The main experimental process involved the insertion of lithium into electrolytic manganese dioxide with glucose as a mild reductant in an autoclave. Both the hydrothermal temperature and the presence of glucose play the critical roles in determining the final spinel integrity. Particular electrochemical performance has also been systematically explored, and the results show that Al^{3+}, F^{-} co-substituted spinels have the best combination of initial capacity and capacity retention among all these samples, exhibited the initial capacity of 115 mAh/g and maintained more than 90% of the initial value at the 50th cycle.

Keywords: Spinel; Hydrothermal reaction; $LiMn_2O_4$; Substitution; Rechargeable batteries

1. Introduction

The increasing demand for portable electronic devices is driving the development of cheap, efficient, compact lightweight and environmental friendly batteries systems. At present, lithium ion batteries tend to be the systems of choice, as they offer higher-energy densities and longer operational life times than most of the other rechargeable battery systems [1]. They are widely incorporated in many electronic types of equipments, such as cellular phones, camcorders and laptop computers.

The first generation of commercial rechargeable lithium ion batteries has been explored by the Sony Corporation in 1991. Such lithium battery has been termed a ''rocking chair'' or ''swing'' battery systems, which consists of layered $LiCoO_2$ as the cathode and graphite as the anode. The high cost and toxicity of cobalt compounds for the cathode of $LiCoO_2$, however, has prompted a search for alternative materials. $LiMn_2O_4$-based spinels offer a potentially attractive alternative to $LiCoO_2$, due to their significant low cost and good safety in comparison to $LiCoO_2$.

In early studies of lithium manganese oxide spinels, these materials exhibited severe capacity fading during charge/discharge cycling, rendering them of less technological interest. One of the main causes for the capacity loss was judged to be the change of a cubic symmetry into a tetragonal one (Jahn–Teller effect) occurring at high reduction levels [2,3]. Subsequently, the basic strategy is an increase of the average Mn oxidation state above 3.5 to reduce the disadvantageous effect. With this aim in mind, many groups have tried to improve spinel cyclability by partly chemical substituting Mn^{3+} with different ions. Recently, Amatucci et al. [4] have pointed out that the combination of anion substitution with cation substitution at the oxygen and the manganese sites, respectively, were quite effective for obtaining both desirable initial capacity and stable cyclability in extensive cycling.

Recently, D. Aurbach group [5–7] has proposed an aqueous reduction of MnO_2 for synthesis of spinel-type lithium manganese oxides. In their process, glucose was

*Corresponding author. College of Chemistry and Chemical Engineering, Lanzhou University, Lanzhou, 730000, PR China.
Tel.: +86 931 8912517; fax: +86 931 8912582.
E-mail address: lihl@lzu.edu.cn (H.-L. Li).

0022-4596/$ - see front matter © 2006 Elsevier Inc. All rights reserved.
doi:10.1016/j.jssc.2006.04.012

employed as a mild reducing agent to enable lithiation of the MnO_2 at relative low temperature, and then upon calcinations, MnO_2 was transformed to highly pure spinel oxides. However, the synthetic route was complicated and the process involved a high-temperature calcinations treatment as a major and critical step. As a preparative method, the hydrothermal process has characteristic features: it enables one to synthesize materials at a far lower temperature [8], and the desired crystalline powders are directly prepared in the hydrothermal treatment. Furthermore, the need for high-temperature calcinations, and subsequent grinding processes are eliminated [9]. Up to date, some research groups have successfully prepared the spinel materials by various hydrothermal procedures [10–14].

In this paper, we have reported a low-temperature hydrothermal synthesis method to prepare a series of spinel-based compounds including cation and/or anion-substituted ones, mainly from commercial lithium and manganese sources. Our aim is to exploit an efficient low-cost and environmental friendly route to prepare spinel-type lithium manganese oxides. The primary studies have mainly focused on investigation of the relationships among the synthesis parameters, structural characteristics and electrochemical performances. The preliminary results have shown that Al^{3+}, F^- co-substituted spinels have the best combination of initial capacity and capacity retention among all these samples, exhibited the initial capacity of 115 mAh/g and maintained more than 90% of the initial value at the 50th cycle.

2. Experimental

2.1. Materials synthesis

All the chemical reagents used in the experiments were A.R., and without further purification. In a typical synthetic process, 0.63 g of $LiOH \cdot H_2O$ (0.0135 mol, 90 wt%), 0.28 g of $Al(NO_3)_3 \cdot 9H_2O$ (0.00075 mol, 99 wt%), and 0.0195 g of LiF (0.00075 mol, 99 wt%) were dissolved in 40 mL of double distilled water. To this solution, 1.33 g of MnO_2 (0.014 mol, 92.6 wt%) was added and the resulting slurry was stirred for 0.5 h at room temperature. Then, 0.1–0.2 g of glucose (0.00055–0.0011 mol, 99 wt%) was added while stirring was in progress, followed by the addition of 40 mL distilled water. This slurry was transferred in a Teflon-lined autoclave of 100 mL volume for hydrothermal treatment. At the end, the reaction was carried out at 200 °C for 24–48 h under an autogeneous pressure. After cooling to room temperature, the solid product was filtered under suction and washed several times with distilled water, then dried at 120 °C for at least 24 h. In addition, a series of lithium manganese oxide samples (summarized in Table 1) were prepared by the hydrothermal method for the aim of comparison. Note that the fluorine stoichiometry is calculated according to the ratio of LiF and EMD in the experimental, and all the discussions on the structural or electrochemical properties of the sample are based on this composition.

2.2. Characterization

Chemical analysis of the spinel samples were conducted by inductively coupled plasma (ICP) technique with the combination of energy-dispersive analysis of X-rays. The average oxidation state of manganese was determined by the chemical redox titration. After the spinel oxide was treated in 0.1 M HNO_3, the obtained reagent was dissolved with H_2O_2 additive. The average valence of Mn ions was determined using Kozawa's methods which is an inverse oxidation–reduction titration using $FeSO_4$ as a reducing agent [11]. The thermal stability of the samples was analyzed using a Perkin–Elmer TG instrument (PE7, USA) in the temperature range from room temperature to 800 °C at a heating rate of 10 °C/min. The morphologies of EMD and the spinel samples were characterized by scanning electron microscopy (SEM) in a JSM 5600LV scanning microscope. Powder X-ray diffraction measurements were performed on a Rigaku diffractometer (D/max-2400, Japan, Cu $K\alpha$ radiation, $\lambda = 1.54178$ Å).

2.3. Electrochemical measurements

Electrode mixtures were prepared by mixing 77% (wt%) active material, 18% acetylene black and 5% polyvinylidene fluoride (PVDF) as binder. After brief evaporation drying, the electrodes were assembled to cells in an argon-filled dry glovebox. The spinel-based compounds were used as the positive electrode, Li metal disk as the negative electrode, and Celgard 2400 membrane was used as the

Table 1
Synthesis conditions of the spinel samples prepared in this work

Sample	Starting materials	Synthesis	Temperature (°C)	Composition[a]
A	MnO_2 LiOH	Without glucose	200	Mainly MnO_2
B	MnO_2 LiOH	With glucose	100	MnO_2 and $Li_{0.94}Mn_2O_4$
C	MnO_2 LiOH	With glucose	200	$Li_{0.94}Mn_2O_4$
D	MnO_2 LiOH $Al(NO_3)_3$ LiF	With glucose	200	$Li_{0.94}Al_{0.1}Mn_{1.9}O_{4-x}F_x$ $(0<x<0.1)$
E	MnO_2 LiOH $Al(NO_3)_3$	With glucose	200	$Li_{0.94}Al_{0.1}Mn_{1.9}O_4$

[a]The average oxidation state of manganese was determined by the chemical redox titration and the corresponding fluorine stoichiometry is calculated according to the ratio of LiF and EMD in the experimental.

separator. The electrolyte was based on 1 M $LiPF_6$ in a 1:1 (volume ratio) mixture of ethylene carbonate (EC) and dimethyl carbonate (DMC). The electrochemical tests, including cyclic voltammetry and galvanostatic charge/discharge, were carried out on a CHI-660 electrochemical station combined with Land (CT2001A) cell systems. Cyclic voltammetry curves were recorded from 3.0 to 4.5 V at a scan rate of 0.1 mV/s, with Li metal disk served as both counter electrode and reference electrode. Galvanostatic charge/discharge tests were performed at a current density of $C/3$ (C means the discharge rate of 147 mA/g, and the discharge rate of $C/3$ is 49 mA/g), in the voltage range of 3.0 to 4.4 V.

3. Results and discussion

3.1. Characterization of the powders

In a preliminary study of the thermal behavior of the spinel samples, typical TG data of sample D presented in Fig. 1. A small quantity of weight-loss observations was observed in the TG curve up to 800 °C. Indeed, TG plot showed a progressive weight loss totally of only 1.7%. The distinct weight loss is less than 0.3% at 225 °C, which is probably attributed to the occurrence of structural water content. At a temperature range from 300 °C to 600 °C, it is a gradual weight loss of about 1.4%, accompanying with impurity of starting materials (because of the purity of EMD is about 92.6%) and the decomposition to Mn_2O_3 at about 550 °C [15]. When the temperature rose up to 600 °C, little loss oxygen was observed as reported by the literatures [16,17]. Such trifle weight-loss behavior is clearly different from that of spinel-type lithium manganese oxides prepared by the sol–gel synthesis, in which usually complex chemical and/or physical reactions occur with larger weight losses [18].

To investigate the morphology changes by the hydrothermal procedure, Fig. 2 illustrates the SEM images of the pristine EMD and sample D. As shown in Fig. 2a and 2c, the pristine EMD particles, show block in morphology with irregular dispersion. The average particle size changes from 10 to 50 μm. Comparing Fig. 2a with 2b, it can be found that a fundamental morphology change has taken place. The morphology of the hydrothermal synthesized product turned into small particles. Higher-magnification SEM image (Fig. 2d) further illustrates that the formed spinel oxide exhibits well-dispersed crystalline and the average particle size declined to about 1 μm. It indicated that reasonable crystallized spinel oxide has produced during the special hydrothermal process.

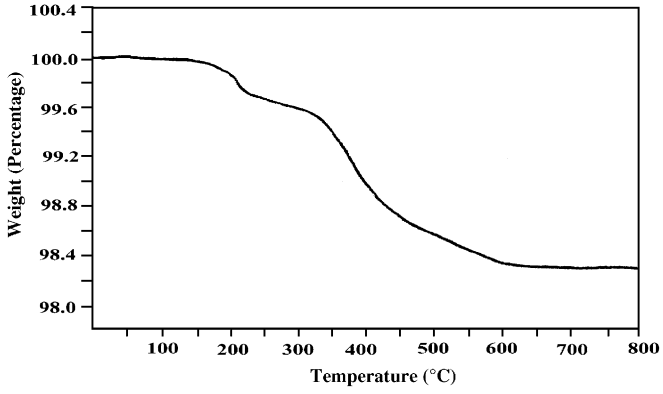

Fig. 1. TG curve of sample D at a heating rate of 10 °C/min.

The XRD patterns of EMD showed in Fig. 3. The patterns reveal that the γ-MnO_2 is a relatively low degree of crystallization with broad, low-intensity peaks, which is well consistent with γ -MnO_2 compounds synthesized by a simple traditional method. In fact, this is a common feature of commercially EMD materials widely used in primary batteries.

The patterns of both sample A and B are very similar to that of the above-discussed pristine EMD, but most peaks continuously shifted toward a lower diffraction angle. This feature confirms that lithium intercalation has occurred in the EMD in a topotactic manner without much disturbance in its structure. In addition, a minor amount of spinel-$LiMn_2O_4$ can also be found in Fig. 3c, suggesting lithium manganese oxides have been initially formed by the hydrothermal method at 100 °C [5].

Upon further hydrothermal treatment, it could be seen from sample C, the diffraction peaks can be assigned to the well-known spinel phase (PDF#350782), with an $Fd3m$ space group. The lattice constant of this material, a_0, on the basis of a least-squares program are listed below:

$$A = \frac{\sum_{i=1}^{n}\delta_i^2\sum_{i=1}^{n}a_i\sin^2\theta_i - \sum_{i=1}^{n}a\delta_i\sum_{i=1}^{n}\delta_i\sin^2\theta_i}{\sum_{i=1}^{n}a_i^2\sum_{i=1}^{n}\delta_i^2 - \left(\sum_{i=1}^{n}a_i\delta_i^2\right)}, \quad (1)$$

$$a = H^2 + K^2 + L^2, \quad (2)$$

$$\delta = 10\sin^2 2\theta, \quad (3)$$

$$A = \lambda^2/4a_0^2 \quad (4)$$

is calculated to be 0.8219 nm. In the case of samples D and E, all the reflections are identified as a single spinel phase and shifted progressively towards a higher angle, indicating a contraction of the lattice. By calculation, the lattice constant of Al-substituted spinels is 0.8188 nm, a little smaller than that of $LiMn_2O_4$ spinel. It was able to deduce from that Al^{3+} was chosen to substitute Mn^{3+} on the 16d sites (octahedral sites), corresponding to increasing the average valence of Mn ions achieved in the prepared sample. Since the ionic radius of Mn^{4+} (0.53 Å) and Al^{3+} (0.53 Å) is smaller than that of Mn^{3+} (0.65 Å), it results in the smaller lattice parameter. Compared with Al-doped spinel, the lattice constant was found to be 0.8197 nm with the use of monovalent fluorine substituted for divalent oxygen. This trend is opposite to what is expected by Vegard's rule for the substitution of O for smaller F anion. Therefore, the increase in crystal lattice parameter can be assumed to originate in the increase quantity of larger trivalent manganese, due to charge compensation relative

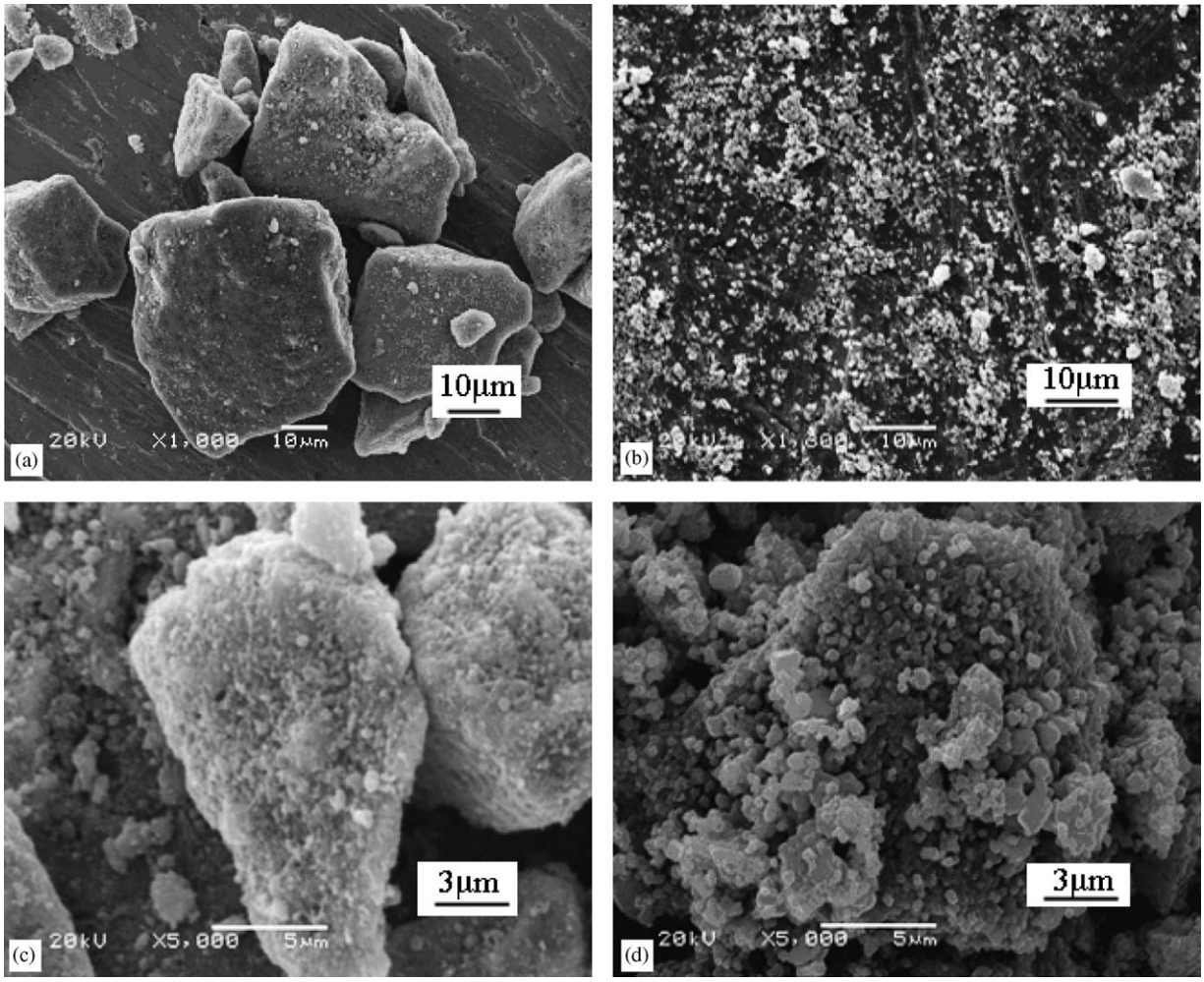

Fig. 2. SEM images of (a) and (c): EMD; (b) and (d): sample D.

to the substitution of fluorine ions for oxygen ions in the cubic structure. Accordingly, the substituted spinel structure can be described as ideally consisting of a cubic close-packing arrangement, lithium ions basically occupy the tetrahedral 8*a* sites, Al and Mn ions in the octahedral 16*d* sites, and F, O ions at the 32*e* sites; the 8*b*, 48*f*, and 16*c* sites remain empty.

Summarizing the structural changes revealed by XRD, it is clear that a very substantial difference occurs when using glucose as a reductant. The main peaks have progressively become obvious with increasing the temperature. With the combination of the above TG result, it reveals that the one-step hydrothermal reaction at 200 °C and using glucose are perfectly adapted to obtain pure and reasonable crystallized spinels.

3.2. Electrochemical performance

Fresh electrodes of the selective samples and pristine EMD, possessing a similar amount of active masses, were fabricated and characterized by cyclic voltammetry (CV), as shown in Fig. 4. For all the voltammograms, the cell voltage was scanned from 3.0 to 4.5 V at a scan rate of 0.1 mV/s. In Fig. 4, sample C appeared two pairs of redox peaks, which are located around 3.95, 4.04 V and 4.07, 4.18 V, which can be associated with the reversible oxidation and reduction reactions corresponding to lithium extraction and insertion [19]. As was earlier reported by Tarascon and Guyomard [20,21], the two reduction and two oxidation peaks represent that the insertion and extraction of lithium ions, respectively, and each occurs in two stages. For example, the first and the second reduction peaks are also assigned to equilibrium between $LiMn_2O_4$–$Li_{0.5}Mn_2O_4$ and $Li_{0.5}Mn_2O_4$–λ-MnO_2. Simultaneity, the cathodic/anodic peaks of $LiMn_2O_4$ are sharpened and show well-defined splitting, which is a characteristic of the Li ion with a high degree of diffusion.

For sample D, both pairs of the anodic and cathodic peaks are shifted slightly to positive potential (about 0.05–0.1 mV). Also, the anodic and cathodic peak currents around 4.1 V for Al^{3+}, F^- co-substituted spinels are smaller than those for $LiMn_2O_4$. It is clear that the shape (i.e., position of the peaks and their height) of the CV is affected by the introduction of the dopant. This may induce the insertion/extraction of Li ions partly in a single-phase process without undergoing a two-phase reaction

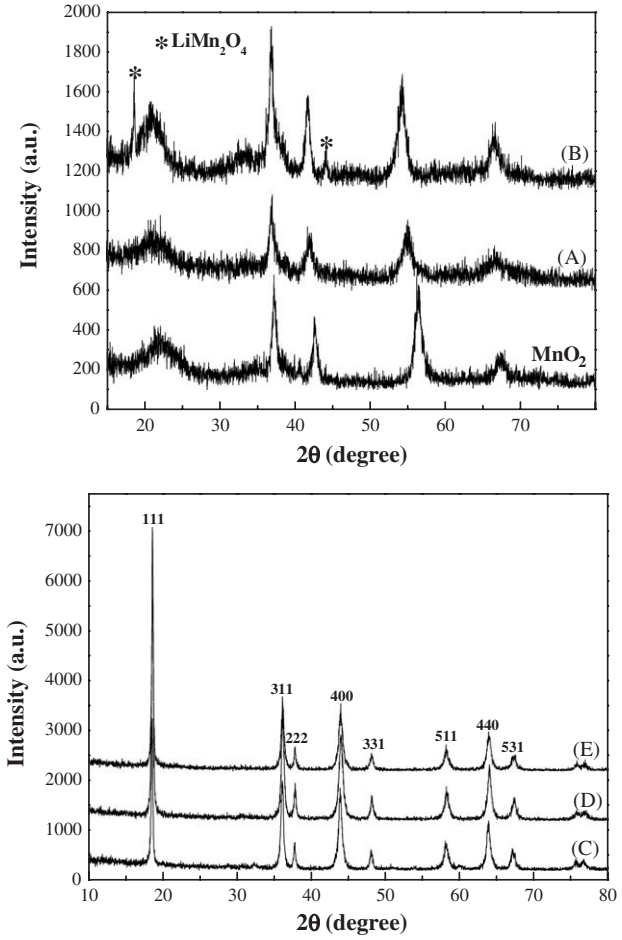

Fig. 3. XRD patterns of EMD and the samples.

between the unstable cubic $Li_{0.5}Mn_2O_4$ and λ-MnO_2 at 4.1 V during the electrochemical cycling [22].

Contrary to the samples of 200 °C, the EMD electrode shows very low current density in the voltage range, reflecting its low initial activity associated with lithium insertion–deinsertion. According to the CV curve, the characteristic of EMD is distinguished from that of spinel-$LiMn_2O_4$ and more likely an electrochemical capacitive behavior, in which case the CV curve is close to ideal rectangular shape. To evaluate the effect of reaction temperature and reductant, the CV plots of samples A and B were also studied. It is noticed that neither hydrothermal treatment at 100 °C nor without using glucose shows distinct cathode/anode peaks in the CV. The reactive performances of the two samples over its pristine counterpart could not be greatly changed, as the powder XRD patterns are more or less similar. Only sample B, the two pairs of faint redox peaks which are a characteristics of spinel-type are detectable.

Based on the above discussions, we have concluded that both glucose and reactive temperature play very critical roles in the formation of pure and reasonable crystallized spinels. It is generally known that the pristine EMD correlating with γ-MnO_2 consists of a random intergrowth of ramsdellite (2×1 channels) and pyrolusite (1×1 channels) structure. The larger channels of the ramsdellite structure make it a host material possible to accommodate lithium insertion/extraction. Under the hydrothermal conditions, the reduction process of EMD by the mild reagent of glucose was developed in aqueous medium. Due to the presence of charge equilibrium, Li^+ may diffuse into the mixed structure through the channel space, and react with negatively charged MnO_2. Then, at the appropriate hydrothermal temperature, the new born lithiated MnO_2 [5] (it means lithium ion has inserted into the channel structure of γ-MnO_2), an intermediate product will undergo with a local rearrangement of atomic structure in the autoclave, resulting in the formation of a reassembled spinel compound.

The specific capacity and cyclability of the products were determined by galvanostatic charge–discharge measurements at a current density of 49 mA/g between cutoff voltages of 3.0 and 4.4 V. As shown in Fig. 5, it is significant that, the first discharge curve of the pristine EMD displays a complete redox process, which is taking place along a continuous voltage decrease without a marked plateau. This fact indicates that the charge/discharge mechanism does not proceed via a two-phase reaction, instead, is a case for the complex one-phase spinel system [23].

It is significant that another discharge curves show two plateaus separated by about 100 mV between the cutoff voltages. This two-plateau feature is particularly distinct from pure $LiMn_2O_4$ phase, which is well consistent with the two pairs redox peaks observed in the cyclic voltammetry experiments. The initial discharge capacity of sample C (109 mAh/g) was 9 mAh/g higher than that of sample E (100 mAh/g). The lower Mn^{3+} content with respect to doped spinel explains the initially lower capacities, since only Mn^{3+} contributes to the electrochemical reaction in this potential range. For sample D, it delivers the initial capacity of 115 mAh/g, which is the highest value among all these samples. Using monovalent fluorine substitution for divalent oxygen increases the amount of Mn^{3+} content available for redox, thereby enhances the specific capacity.

The cycle life data in the 4 V region for the spinel phase along with pristine MnO_2 are shown in Fig. 6. The initial capacity of the pristine MnO_2 for Li insertion and extraction is very low (considering it could not be completely cathodic polarized in this potential range), and maintains extremely stable under extensive cycling. Although sample C exhibits a relatively high initial capacity that then fades substantially with a capacity loss over 30 cycles of over 0.8% per cycle. It is well known that stable capacity retention is a key property in designing materials in this field. Just as many research groups mentioned [4], doping Al element was expected to enhance the cyclability in comparison to that of the patent $LiMn_2O_4$. In Fig. 6, spinel-type $LiMn_2O_4$ with a trace of Al substitution has been better cycling performance with a

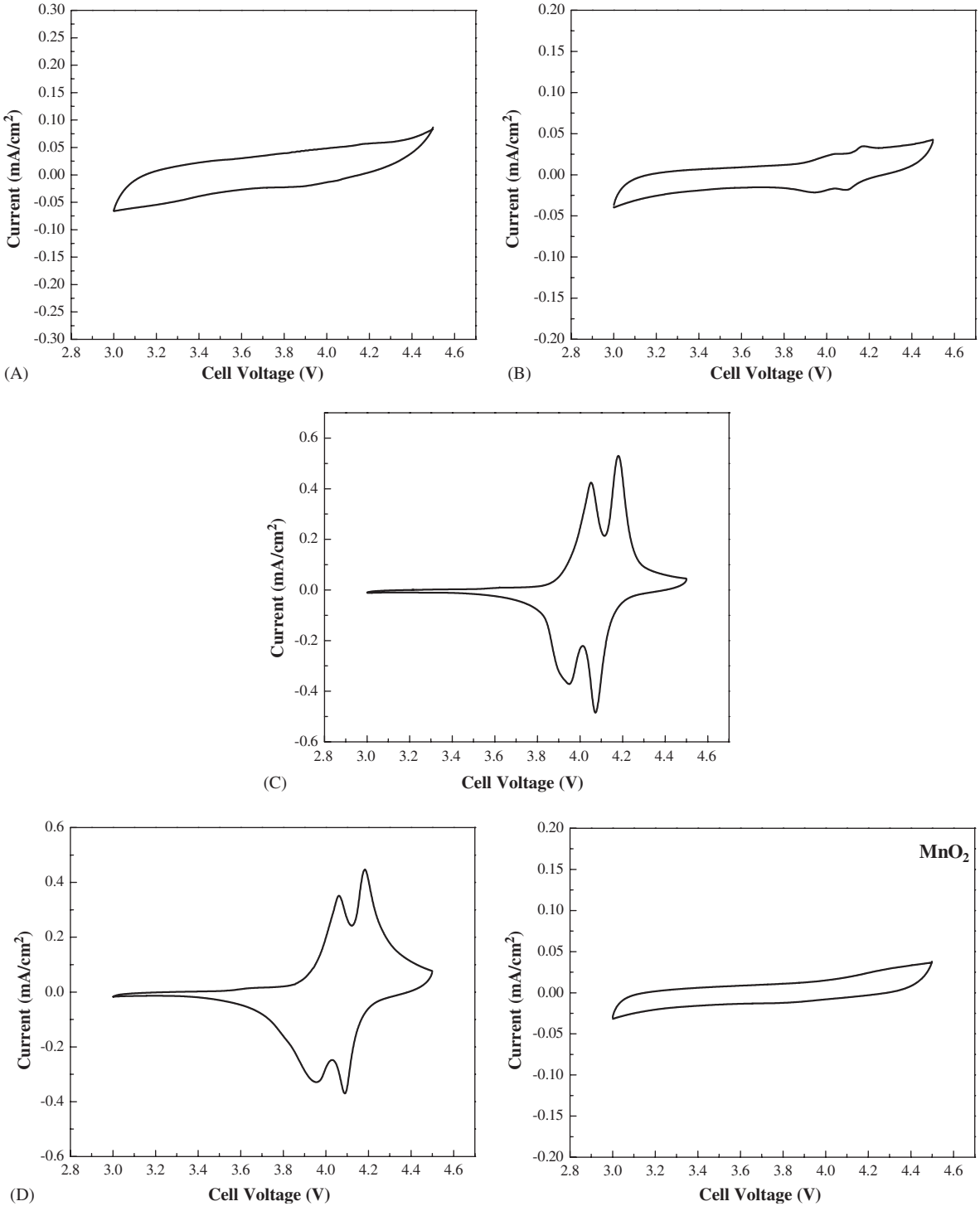

Fig. 4. Cyclic voltammograms of EMD and the samples, in the potential range 3.0–4.5 V vs. Li/Li^+, at a scan rate of 0.1 mV/s.

capacity loss over 30 cycles of less than 0.4% per cycle. And Al^{3+}, F^- co-substituted spinel-type $LiMn_2O_4$, in particular, has maintained more than 90% of the initial value at the 50th cycle. This result is considerable to that of D. Aurbach group results about the calculated spinels discharged at 10 mA/g, where the initial capacity was 116 mAh/g and declined to 107 mAh/g at the 50th cycle.

It is evident from the above results that even substitutional level as low as 0.1 atom/formula unit produces structural effects that are reflected in the electrochemical characteristics. Thackeray [24] described that the cyclability of lithium secondary batteries depended greatly on the structural integrity of the host materials during charge and discharge. It was thought that Al-doped samples are more

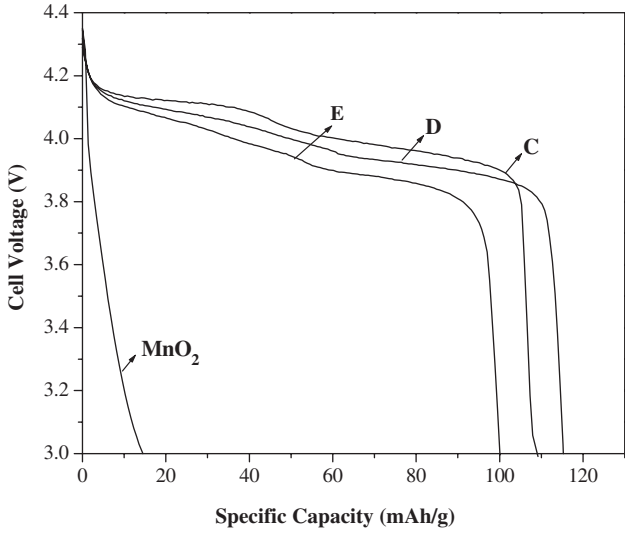

Fig. 5. The first cycle discharge curve of EMD and the samples, in the potential range 3.0–4.4 V vs. Li/Li^+, at a current density of 49 mA/g.

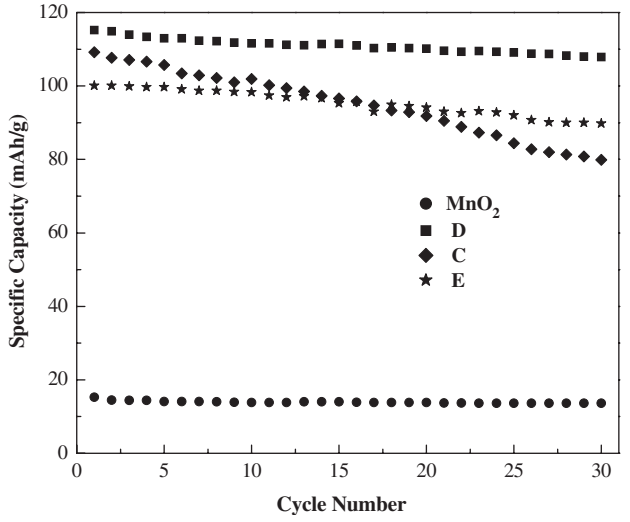

Fig. 6. Specific discharge capacities vs. cycle number, in the potential range 3.0–4.4 V vs. Li/Li^+, at a current density of 49 mA/g.

stable than undpoed ones, according to the stand Gibbs free energies of the formation at 298 K, i.e., Al_2O_3 (−1573 KJ/mol), Mn_2O_3 (−881 KJ/mol). Hence, it is reasonable to think that the bonding of Al–O is much stronger than Mn–O. This means that the expansion or contraction of the spinel structure with intercalation/deintercalation of lithium ions may be restricted by the Al^{3+} substitution, suggesting the lattice stabilization should be achieved in this Al-doped spinels. On the other hand, elimination of any trace gradient-induced cooperative Jahn–Teller distortion will be effective in improving the capacity retention. Obviously, aluminum has a small ionic size, 0.53 Å, which restricts the dynamic Jahn–Teller Mn^{3+} cations from forming a cooperative c/a expansion and reduces strains on the lattice during repeated cycling. Namely, the Al-doped spinels with a smaller lattice are more resistant against the volume change, which eventually give rise to a better cycling performance.

4. Conclusion

We have proposed an elegant approach that can directly lead to potentially useful spinel-based materials by the hydrothermal process. Moreover, the simple reaction has mainly utilized electrolytic manganese dioxide and lithium hydroxide, which are the cheapest manganese and lithium sources, and glucose as the mild reductant in an autoclave. XRD results have clearly revealed that both glucose and reactive temperature play critical roles in determining the final spinel structure. Electrochemical testing of these materials as the active mass for Li-ion batteries has shown that F^- and Al^{3+} co-substituted spinel sample is superior to the undoped lithium manganese oxide, particularly in increasing the initial capacity and retaining the stable cyclability aspects. We believe that the approach we outline herein is a simple, cost-effective and environmental friendly method to synthesize of spinel-$LiMn_2O_4$, it is preferable to the classical solid-state reaction in terms of saving time and the energy. Future research is currently in progress to optimize the cathode composition and microstructure, particularly to increase the initial capacity and enhance cyclability at elevated temperature.

References

[1] J. Kim, A. Manthiram, Nature 390 (1997) 265.
[2] A. Yamada, K. Miura, K. Hinokuma, M. Tanaka, J. Electrochem. Soc. 142 (1995) 2149.
[3] T. Ohzuku, J. Kato, K. Sawai, T. Hirai, J. Electrochem. Soc. 138 (1991) 2556.
[4] G.G. Amatucci, N. Pereira, T. Zheng, I. Plitz, J.M. Tarascon, J. Power Sources 81–82 (1999) 39.
[5] V. Ganesh Kumar, J.S. Gnanaraj, S. Ben-David, D.M. Pickup, E.R.H. van-Eck, A. Gedanken, D. Aurbach, Chem. Mater. 15 (2003) 4211.
[6] A. Odani, A. Nimberger, B. Markovsky, E. Sominski, E. Levi, V.G. Kumar, A. Motiei, A. Gedanken, P. Dan, D. Aurbach, J. Power Sources 119 (2003) 517.
[7] V.G. Kumar, J.s. Gnanaraj, G. Salitra, A. Abramov, A. Gedanken, D. Aurbach, J.B. Soupart, J.C. Rousche, J. Solid State Electrochem. 8 (2004) 957.
[8] M. Yoshimura, J. Mater. Res. 13 (1998) 769.
[9] Y.C. Zhang, H. Wang, H.Y. Xu, B. Wang, H. Yan, A. Ahniyaz, M. Yoshimura, Solid State Ionics 158 (2003) 113.
[10] K. Kanamura, K. Dokko, T. Kaizawa, J. Electrochem. Soc. 152 (2005) A395.
[11] T. Kanasaku, K. Amezawa, N. Yamamoto, Solid State Ionics 133 (2000) 51.
[12] Q. Feng, H. Kanoh, Y. Miyai, K.Ooi J. Electrochem. Soc. 7 (1995) 1226.
[13] S.T. Myung, S. Komaba, N. Kumagai, Electrochim. Acta 47 (2002) 3287.
[14] Y. Wang, S. Nishiuchi, T. Kuroki, High Pressure Res. 20 (2002) 299.
[15] R. Dziembaj, M. Molenda, J. Power Sources 119–121 (2003) 121.
[16] Y. Gao, J.R. Dahn, J. Electrochem. Soc. 143 (1996) 1783.

[17] L. Hernán, J. Morales, L. Sánchez, J. Santos, Solid State Ionics 104 (1997) 205.
[18] S.J. Bao, Y.Y. Liang, W.J. Zhou, B.L. He, H.L. Li, J. Colloid, Interface Sci. 291 (2005) 433.
[19] W. Liu, G.C. Farrington, F. Chaput, B. Dunn, J. Electrochem. Soc. 143 (1996) 879.
[20] D. Guyomard, J.M. Tarascon, J. Electrochem. Soc. 139 (1992) 937.
[21] J.M. Tarascon, D. Guyomard, J. Electrochem. Soc. 138 (1991) 2864.
[22] K.W. Kim, S.W. Lee, K.S. Han, H.J. Chung, S.I. Woo, Electrochim. Acta 48 (2003) 4223.
[23] Y.L. Lu, M. Wei, Z.Q. Wang, D.G. Evans, X. Duan, Electrochim. Acta 49 (2004) 2361.
[24] M.M. Thackeray, J. Electrochem. Soc. 142 (1995) 2558.